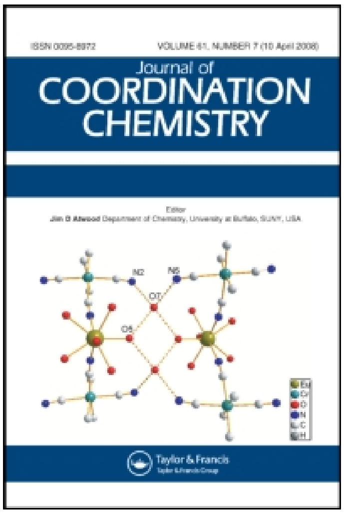

Journal of Coordination Chemistry
Publication details, including instructions for authors and subscription information:
http://www.informaworld.com/smpp/title~content=t713455674

Synthesis, spectra and crystal structure of a dinuclear manganese(χ) complex $[(NTB)Mn(\mu\text{-}O)]_2(ClO_4)_4 \cdot 2H_2O$

Feng-Ping Xiao[a,b]; Bi-Bo Yu[b]; Zhan-Ru Liao[b]
[a] College of Chemistry and Molecular Science, Wuhan University, Wuhan, Hubei, P.R. China [b] School of Chemistry, Central China Normal University, Wuhan, P.R. China

First published on: 19 September 2007

To cite this Article Xiao, Feng-Ping , Yu, Bi-Bo and Liao, Zhan-Ru(2008) 'Synthesis, spectra and crystal structure of a dinuclear manganese(χ) complex $[(NTB)Mn(\mu\text{-}O)]_2(ClO_4)_4 \cdot 2H_2O$', Journal of Coordination Chemistry, 61: 3, 384 — 391, First published on: 19 September 2007 (iFirst)

To link to this Article: DOI: 10.1080/00958970701338465

URL: http://dx.doi.org/10.1080/00958970701338465

Journal of Coordination Chemistry
Vol. 61, No. 3, 10 February 2008, 384–391

Taylor & Francis
Taylor & Francis Group

Synthesis, spectra and crystal structure of a dinuclear manganese(χ) complex $[(NTB)Mn(\mu\text{-}O)]_2(ClO_4)_4 \cdot 2H_2O$

FENG-PING XIAO*†‡, BI-BO YU‡ and ZHAN-RU LIAO*‡

†College of Chemistry and Molecular Science, Wuhan University, Wuhan,
Hubei 430072, P.R. China
‡School of Chemistry, Central China Normal University,
Wuhan 430079, P.R. China

(*Received 22 December 2006; in final form 26 January 2007*)

A novel dinuclear manganese(χ) complex $[(NTB)Mn(\mu\text{-}O)]_2(ClO_4)_4 \cdot 2H_2O$ (**1**) (NTB = tris(2-benzimidazolylmethyl) amine) has been synthesized and characterized. The crystal structure is determined by single crystal X-ray diffraction. The compound crystallizes in the monoclinic system, space group $C2/c$ with $a = 18.3461(1)$, $b = 15.4170(1)$, $c = 21.0141(1)$ Å, $\beta = 90.5290(1)°$, $V = 5943.4(8)$ Å^3, $Z = 4$ and $R_1 = 0.0789$ for 5729 observed reflections. Two manganese atoms are bridged by two oxygen atoms forming a dinuclear complex. The results of interaction between **1** and H_2O_2 indicated that hydrogen peroxide destroyed the Mn_2O_2 unit of **1**.

Keywords: Dinuclear manganese; Synthesis; Crystal structure; Model complex

1. Introduction

A by-product of aerobic respiration hydrogen peroxide in the presence of reducing metals Fe(χ) or Cu(χ) can be converted to hydroxyl radicals whose deleterious effects on cell components is well documented [1, 2]. Catalase enzymes are able to disproportionate H_2O_2 into dioxygen and water [3] and play a vital role in the protection of living cells against oxidative stress by eliminating hydrogen peroxide before its reduction gives rise to hydroxyl radical [4]. Some catalases contain dinuclear manganese activity sites to catalyze the dismutation of H_2O_2 [3a, 5]. Several crystal structures are available for manganese catalase (MnCat), including two at atomic resolution [6]; a number of structural model complexes have been synthesized and studied [7].

EPR, UV-visible spectroscopy, and X-ray absorption spectroscopy have shown that MnCat can exist in at least four states of these: a reduced Mn_2^{χ} state, a mixed-valence $Mn^{\chi}Mn^{\chi}$ state, an oxidized Mn_2^{χ} state, and a superoxidized $Mn^{\chi}Mn^{\chi}$ state [8].

---

*Corresponding authors. Email: fengpingxiao@163.com; zhanruliao@163.com

Journal of Coordination Chemistry
ISSN 0095-8972 print/ISSN 1029-0389 online © 2008 Taylor & Francis
DOI: 10.1080/00958970701338465

But, there is a lack of the reactivity of a $\mathrm{Mn}^{\chi}\mathrm{Mn}^{\chi} \leftrightarrow \mathrm{Mn}^{\chi}\mathrm{Mn}^{\chi}$ catalytic cycle. Spectroscopic studies have indicated that H_2O_2 can both oxidize the reduced enzyme and reduce the oxidized enzyme. The mixed-valance $\mathrm{Mn}^{\chi}\mathrm{Mn}^{\chi}$ oxidation state is the least well characterized, and the *L. plantarum* enzyme has not been shown to form a stable mixed-valence $\mathrm{Mn}^{\chi}\mathrm{Mn}^{\chi}$ form. On the basis of model studies [9], the $\mathrm{Mn}^{\chi}\mathrm{Mn}^{\chi}$ derivative is formed by one-electron reduction of the oxidized enzyme by NH_2OH and is then oxidized by H_2O_2 to form the inactive, superoxidized $\mathrm{Mn}^{\chi}\mathrm{Mn}^{\chi}$ enzyme.

Model complexes of manganese catalase including *bis*-μ-oxo dimanganese complexes have been studied [7(d), 10]. Higher valent Mn_2^{χ} (μ-O)$_2$ complexes have been prepared with a multitude of supporting ligands [11]. Despite variation in ligands, these complexes show a typical Mn–Mn separation of 2.7 ± 0.1 Å [12]. UV-Vis spectroscopy is a particularly good technique for understanding electronic structure of Mn^{χ} and Mn^{χ} complexes which usually exhibit d–d and charge transfer absorption bands in visible and high energy bands [13].

In this article, as parts of our synthetic explorations of $[(\mathrm{NTB})\mathrm{Mn}(\mu\text{-O})]_2(\mathrm{ClO_4})_4 \cdot 2H_2O$ (**1**), the synthesis, spectra and crystal structure of it have been studied. The ligand was prepared according to an improved method with ethylene glycol solvent [14, 15].

2. Experimental

2.1. *Preparation of* $[(\mathrm{NTB})\mathrm{Mn}(\mu\text{-O})]_2(\mathrm{ClO_4})_4 \cdot 2H_2O$ *(1)*

To solution of NTB (0.815 g, 2 mmol) in absolute ethanol (25 mL) was added $\mathrm{Mn(ClO_4)_2} \cdot 6H_2O$ (0.730 g, 2 mmol) dissolved in water (3 mL). The mixture was stirred 15 min at 50°C, then malonic acid (0.104 g, 1 mmol) was added. The color of the solution changes from colorless to black-green with a little black-green precipitate. After 4 h, the resulting precipitate was filtered off, washed with absolute ethanol and dried under IR light. The powder was dissolved in acetonitrile and some unexpected crystals were grown at room temperature by the diffusion of acetonitrile to diethyl ether in one day with yield: 1.1 g (77%).

2.2. *Physical measurements*

IR spectra were recorded on an AVATAR 360 FT-IR spectrophotometer. UV-Vis spectra were recorded on a Shimadzu-UV-2501 spectrophotometer. Elemental analyses were performed on a Perkin-Elmer 2400 CHN elemental analytical instrument for C, H, N and Perkin-Elmer OPTIMA 2000 DV optical emission spectrometer for Mn. Anal. Calcd for $C_{48}H_{50}Cl_4Mn_2N_{14}O_{22}$ (1426.70): C 40.41, H 3.53, N 13.75, Mn 7.70%. Found: C 40.66, H 3.48, N 13.83, Mn 7.75%. IR (KBr, cm^{-1}): 3357 br (νNH), 3300–3200 br (νOH), 1624 (δ–C–H), 1450 (δ–CH$_2$–), 1326 (νC–N), 748 (δ arC–H), 626 (νMn–O), 526 (νMn–N). UV-Vis (acetonitrile, nm) [$\lambda_{\max}(\varepsilon)$, L mol^{-1} cm^{-1}]: 288 (1.80×10^4), 390 (3.62×10^3), 558 (1.23×10^3), 655 (1.16×10^3).

2.3. *Crystallographic data*

A small black-green crystal was mounted on a thin glass fiber for X-ray diffraction data collection. Intensity data were collected with graphite monochromatic Mo-Kα radiation ($\lambda = 0.71073$ Å) at 292(3) K on a Bruker Smart APEX diffractometer. From a total of 17594 reflections corrected by SADABS [16, 17] in the $1.94 \leq \theta \leq 27.50^\circ$ range, 6776 were independent with $R_{\text{int}} = 0.0613$, of which 3610 observed reflections with $I > 2\sigma(I)$ were used in the structural analysis. The structures were solved by direct methods and all non-hydrogen atoms were refined with anisotropic thermal parameters. All hydrogen atoms were located in calculated positions and/or in the positions from difference Fourier map. The positions and anisotropic differences of non-hydrogen atoms were refined on F^2 by full-matrix least-squares techniques with *SHELXTL* program package [17, 18]. The crystallographic data are given in table 1. Difference electron density maps revealed the presence of disordered lattice solvate water and perchlorate ions, and among them atom C12 were constrained with special positions of $x = 0.5000$, $z = 0.2500$, U23 = 0, U12 = 0, sof = 0.5; atom O6 with $x = 0.5000$, $z = 0.2500$, U23 = 0.7500, sof = 0.5; and atom O9 with sof = 0.4.

3. Results and discussion

3.1. *Synthesis of (1)*

Due to the half-full d orbit in Mn(χ) ions, it is difficult to oxide the manganese(χ) salts to high valence manganese compounds in normal reactive condition. However, in the

Table 1. Crystal data of $[(\text{NTB})\text{Mn}(\mu\text{-O})]_2(\text{ClO}_4)_4 \cdot 2\text{H}_2\text{O}$.

Empirical formula	$C_{48}H_{42}Mn_2N_{14}O_2 \cdot (ClO_4)_4 \cdot (H_2O)_4$
Formula weight	1426.70
Temperature (K)	293(2)
Wavelength (nm)	0.071073
Crystal system	Monoclinic
Space group	*C2/c*
a (Å)	18.3461(1)
b (Å)	15.4170(1)
c (Å)	21.0141(1)
α (°)	90
β (°)	90.5290(1)
γ (°)	90
V (Å^3)	5943.4(8)
Z	4
Calculated density (g cm^{-3})	1.594
Linear absorption coefficient (mm^{-1})	0.695
F(000)	2920
Crystal size (mm^{-3})	0.24 × 0.20 × 0.10
θ range for data collection (°)	1.94, 27.50
Reflections collected	17594
Independent reflections	6776
Refinement method	Full-matrix least-squares on F^2
Goodness-of-fit on F^2	1.018
Final *R* indices [$I > 2\sigma(I)$]	$R_1 = 0.0789$, $wR_2 = 0.2205$
R indices	$R_1 = 0.1153$, $wR_2 = 0.2548$
Largest diff. peak and hole (e Å^{-3})	0.702 and −0.762

preparation of **1**, aerial dioxygen acts as oxidant (equation 1). Maybe malonic acid in the synthesis of **1** acts as a pH regulator or catalyst.

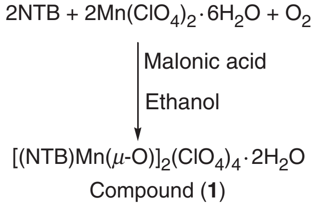

$$2\mathrm{NTB} + 2\mathrm{Mn(ClO_4)_2\cdot 6H_2O} + \mathrm{O_2} \xrightarrow[\text{Ethanol}]{\text{Malonic acid}} [(\mathrm{NTB})\mathrm{Mn}(\mu\text{-O})]_2(\mathrm{ClO_4})_4\cdot 2\mathrm{H_2O}$$

Compound (**1**)

3.2. *IR and UV-Vis spectra*

In the infrared spectrum of **1**, three new strong peaks at 1090, 697 and 626 $\mathrm{cm^{-1}}$ are observed compared to the NTB ligand. The peak at 697 $\mathrm{cm^{-1}}$ is a vibrational mode associated with the $\mathrm{Mn_2^{\chi}O_2}$ core; similar peaks are observed in other di-μ-oxo bridging group complexes [19]. The peak at 1090 $\mathrm{cm^{-1}}$ is assigned to perchlorate uncoordinated with metal. The band at 626 $\mathrm{cm^{-1}}$ is attributed to Mn–O linkages, and the band at 560 $\mathrm{cm^{-1}}$ is assigned to M–N linkages [20].

UV-Vis spectroscopy of the title complex in acetonitrile is characteristic of $[\mathrm{Mn}(\mu\text{-O})]_2^{4+}$ unit. The complex exhibits absorptions at high-energy 390 nm, and low energy 558 and 655 nm. Peaks and intensities are about equal to corresponding peaks in other $\mathrm{Mn_2^{\chi}}$ dinuclear compounds (411 nm, $\varepsilon = 3956\ \mathrm{L\,mol^{-1}\,cm^{-1}}$; 544 nm, 843; 632nm, 657) [21]. The absorptions at 390 and 655 nm were attributed to μ-oxo to Mn(χ) d_{π} charge-transfer transitions [22]. The absorptions at 558 nm may be assigned to d–d transition of Mn(χ) cations, similar bands were reported for tpen and phen dimers and assigned to d–d transitions [22, 23]. The extinction coefficient ε of these peaks in the title compound is larger than for $\mathrm{Mn^{\chi}Mn^{\chi}}$ and $\mathrm{Mn_2^{\chi}}$ complexes, attributed to empty d orbitals of the manganese(χ) ions that are prone to accept the p electrons from ligands.

3.3. *Crystal structure*

Complex **1** crystallizes in the monoclinic system and space group *C2/c*. The structure is dinuclear and figure 1 shows the cation $[(\mathrm{NTB})\mathrm{Mn}(\mu\text{-O})]_2^{4+}$; figure 2 is the packing diagram. Selected bond lengths and angles are listed in table 2.

In the structure, each manganese is bonded by four nitrogen atoms from a coordinated NTB ligand (three coming from benzimidazolyl groups and another from alkylamine) and two μ-bridge oxygens in a distorted octahedron. This coordination produces geometric distortions from the ideal octahedron manifest in N–Mn–N bond angles (N2–Mn1–N4, 84.62(1)°; N2–Mn1–N6, 85.71(1)°; N4–Mn1–N6, 154.48(1)°; N6–Mn1–N1, 77.26(1)°) and also between two oxygen atoms (O1–Mn1–O1A, 86.68(9)°). Two manganese atoms and two bridging oxygens are in same plane. The Mn–Mn distance of 2.636 Å is consistent with value observed in manganese complexes adopting the same core. Moreover, as observed from figure 1, the Mn–N bond distances of the NTB ligand are different. The largest corresponds to the Mn–N aliphatic bond (Mn1–N1, 2.185(3) Å), while the three shorter correspond to the Mn–N aromatic bonds (Mn1–N2, 2.034(3) Å;

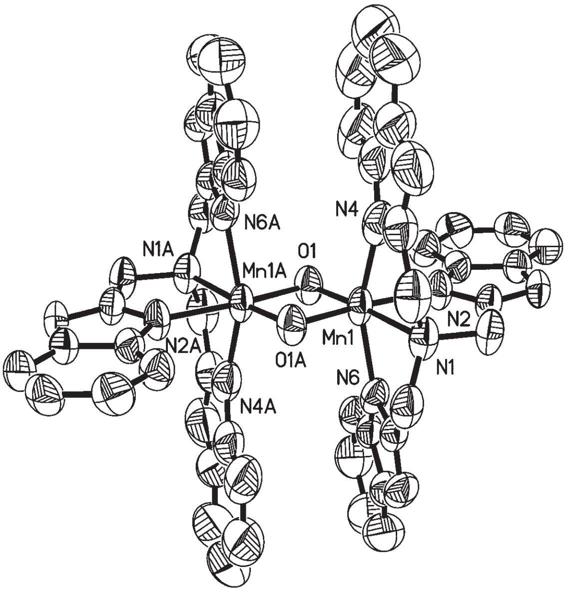

Figure 1. The molecular structure of **1**, showing 50% probability displacement ellipsoids. All hydrogen atoms, solvent molecules and perchlorate ions have been omitted for clarity.

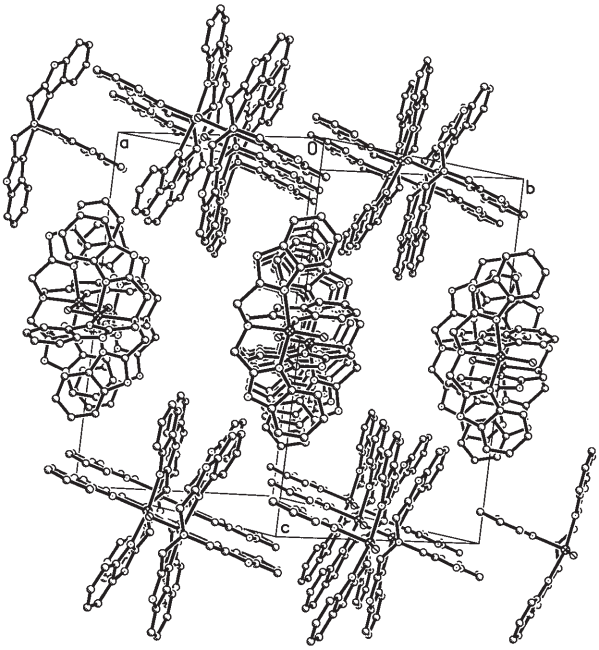

Figure 2. Packing diagram of **1**. All hydrogen atoms, solvent molecules and perchlorate ions have been omitted for clarity.

Table 2. Selected bond lengths (Å) and angles (°) of $[(NTB)Mn(\mu\text{-}O)]_2(ClO_4)_4 \cdot 2H_2O$.

Mn(1)–O(1)	1.798(2)	Mn(1)–O(1)′	1.827(2)
Mn(1)–N(2)	2.034(3)	Mn(1)–N(4)	2.076(4)
Mn(1)–N(6)	2.079(3)	Mn(1)–N(1)	2.185(3)
O(1)–Mn(1)–O(1)	86.68(9)	O(1)–Mn(1)–N(2)	100.44(10)
O(1)–Mn(1)–N(4)	104.65(12)	N(2)–Mn(1)–N(4)	84.62(12)
O(1)–Mn(1)–N(6)	100.31(11)	N(2)–Mn(1)–N(6)	85.71(11)
N(4)–Mn(1)–N(6)	154.48(12)	O(1)–Mn(1)–N(1)	176.85(11)
N(2)–Mn(1)–N(1)	81.46(10)	N(4)–Mn(1)–N(1)	77.97(12)
N(6)–Mn(1)–N(1)	77.26(11)		

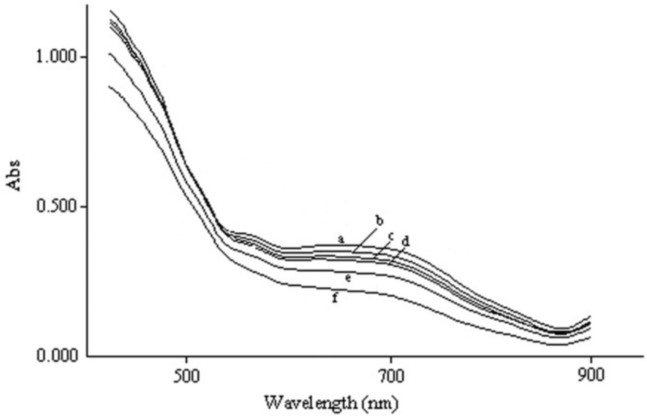

Figure 3. The absorption spectra of the interaction between **1** and H_2O_2. (a) $C_1 = 2.0 \times 10^{-5}$; (b) $C_1 = 2.0 \times 10^{-5}$, $C_{H_2O_2} = 6.6 \times 10^{-6}$; (c) $C_1 = 2.0 \times 10^{-5}$, $C_{H_2O_2} = 1.3 \times 10^{-5}$; (d) $C_1 = 2.0 \times 10^{-5}$, $C_{H_2O_2} = 1.96 \times 10^{-5}$; (e) $C_1 = 2.0 \times 10^{-5}$, $C_{H_2O_2} = 2.5 \times 10^{-5}$; (f) $C_1 = 2.0 \times 10^{-5}$, $C_{H_2O_2} = 3.2 \times 10^{-5}$.

Mn1–N4, 2.076(4) Å; Mn1–N6, 2.079(3) Å). The Mn–O distances of 1.827(2) Å and 1.798(2) Å are shorter than the Mn–N distances.

Intermolecular hydrogen bonds are between the O–H of the solvent water and oxygen from perchlorate ions, and between the N–H of the ligand and the oxygen atoms from perchlorate. The O–H $\cdots$ O hydrogen bond distances range from 2.38(2) to 3.208(9) Å and N–H $\cdots$ O from 2.755(4) to 2.933(13) Å.

3.4. *Interaction between (1) and H_2O_2*

Interaction between **1** and H_2O_2 has been studied using UV-Vis spectra. With increase of the H_2O_2 concentration, the absorption at 558, 655 nm for **1** decreased (see figure 3) and the color of the solution changes to light yellow from green; no oxygen was observed, which may indicate the Mn–O bonds were destroyed and Mn^{χ} ions had been reduced. A drop of triethylamine to the above mixture changed the color from colorless to fawn over time. Comparing to figure 3, the peaks are shifted to 300, 360, 500 nm and the absorptions increased with time (see figure 4). Absorptions at 300 and 360 nm can be assigned to charge-transfer transitions from ligands to manganese ions oxidized by

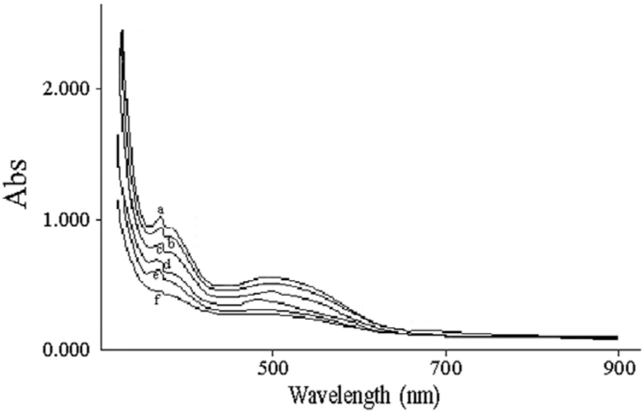

Figure 4. The absorption spectra of the interaction between **1** and H_2O_2 (the original concentration: $C_1 = 2.0 \times 10^{-5}$, $C_{H_2O_2} = 3.2 \times 10^{-5}$) on the presence of triethylamine ($C_{trien} = 2.0 \times 10^{-5}$, t : a = 30, b = 15, c = 8, d = 4, e = 2, f = 1 min).

H_2O_2, possibly indicating that H_2O_2 or H_2O coordinate to manganese ions; it is difficult to reduce the product by H_2O_2 again.

Supplementary material

Crystallographic data for the structure reported in this article have been deposited with the Cambridge Crystallographic Data Centre, CCDC No. 282915. Copies of this information may be obtained free of charge from the Director, CCDC, 12 Union Road, Cambridge CB21EZ, UK (Fax: +44-1223-336-033; E-mail: deposit@ccdc.cam.ac.uk or http://www.ccdc.cam.ac.uk).

References

[1] E.R. Stadtman, B.S. Berlett, P.B. Chock. *Proc. Natl. Acad. Sci. USA*, **87**, 384 (1990).

[2] I. Romero, L. Dubois, M.N. Collomb, A. Deronzier, J.M. Latour, J. Pecaut. *Inorg. Chem.*, **41**, 1795 (2002).

[3] (a) Y. Kono, I. Fridovich. *J. Biol. Chem.*, **258**, 6015 (1983) (b) S.V. Khangulov, V.V. Barynin, S.V. Antonyukbarynina. *Biochim. Biophys. Acta*, **1020**, 25 (1990).

[4] G.C. Dismukes. *Chem. Rev.*, **96**, 2909 (1996).

[5] Y.G. Sheptovitaky, G.W. Brudvig. *Biochemistry*, **37**, 5052 (1998).

[6] (a) V.V. Barynin, P.D. Hempstead, A.A. Vagin, S.V. Antonyuk, W.R. Melik-Adamyn, V.S. Lamzin, P.M. Harrison, P.J. Artymiuk. *J. Inorg. Biochem.*, **67**, 196 (1997); (b) V.V. Barynin, M.M. Whittaker, S.V. Antonyuk, V.S. Lamzin, P.M. Harrison, P. Artymiuk, J.W. Whittaker. *Structure*, **9**, 725 (2001).

[7] (a) B.C. Dave, R.S. Czernuszewicz. *Inorg. Chim. Acta*, **281**, 25 (1998); (b) J. Brinksma, R. Hage, J. Kerschner, B.L. Feringa. *Chem. Commun.*, 537 (2000); (c) S.F. Si, J.K. Tang, D.Z. Liao, Z.H. Jiang, S.P. Yan. *J. Molecular Structure*, **696**, 87 (2002); (d) M.U. Triller, W.Y. Hsieh, V.L. Pecoraro, A. Rompel, B. Krebs. *Inorg. Chem.*, **41**, 5544 (2002).

[8] G.S. Waldo, J. Penner-Hahn. *Biochemistry*, **34**, 1507 (1995).

[9] A. Gelasco, S. Bensiek, V.L. Pecoraro. *Inorg. Chem.*, **37**, 3301 (1998).

[10] A.F. Jensen, Z. Su, N.K. Hansen, F.K. Larsen. *Inorg. Chem.*, **34**, 4244 (1995).

[11] R. Manchanda, G.W. Brudvig, S. Gala, R.H. de Crabtree. *Inorg. Chem.*, **33**, 5157 (1994).
[12] R. Manchanda, G.W. Brudvig, R.H. Crabtree. *Coord. Chem. Rev.*, **144**, 1 (1995).
[13] A.J. Wu, E.J. Penner-Hahn, V.L. Pecoraro. *Chem. Rev.*, **104**, 903 (2004).
[14] H.M.J. Hendriks, J.M.W.L. Birker, J.V. Rijn, G.C. Verschoor, J. Reedijk. *J. Am. Chem. Soc.*, **104**, 3607 (1982).
[15] Z.R. Liao. *J. Chim. Phys.*, **92**, 668 (1995).
[16] G.M. Sheldrick. *SADABS*, University of Göttingen, Germany (1996).
[17] Bruker AXS Inc. *SMART APEX (Version 5.628), SAINT$^+$ (Version 6.45) and SHELXTL-NT (Version 6.12)*, Bruker AXS Inc., Madison, WI, USA (2001).
[18] G.M. Sheldrick. *SHELXS97 and SHELXL97*, University of Göttingen, Germany (1997).
[19] S.R. Cooper, M. Calvin. *J. Am. Chem. Soc.*, **99**, 6623 (1977).
[20] (a) K. Nakamoto. *Infrared and Raman Spectra of Inorganic and Coordination Compounds*, 4th Edn, John Wiley & Sons, New York (1986); (b) S. Lin, S.X. Liu, J.Q. Huang, C.C. Lin. *J. Chem. Soc., Dalton Trans.*, 1595 (2002).
[21] P.A. Goodson, J. Glerup, D.J. Hodgson, K. Michelsen, E. Pedersen. *Inorg. Chem.*, **29**, 503 (1990).
[22] S. Pal, J.W. Gohdes, W.C.A. Wilisch, W.H. Armstrong. *Inorg. Chem.*, **31**, 713 (1992).
[23] M. Stebler, A. Ludi, H.-B. Burgi. *Inorg. Chem.*, **25**, 4743 (1986).